Biophysical Journal, Volume 96

Supporting Material

Mechanisms of ß-adrenergic modulation of I_{Ks} in the guinea-pig ventricle: insights from experimental and model-based analysis

Stefano Severi, Cristiana Corsi, Marcella Rocchetti, and Antonio Zaza

Mechanisms of ß-adrenergic modulation of I_{Ks} in the guinea-pig ventricle: insights from experimental and model-based analysis

Stefano Severi, Cristiana Corsi, Marcella Rocchetti, Antonio Zaza

1. Supplement to Methods

1.1 Myocyte isolation

Hartley guinea-pigs (3-4 months old) were killed by cervical dislocation under combined ketamine (100 mg/kg)-xylazine (5 mg/kg) intraperitoneal anesthesia. Myocytes were dissociated from both ventricles by retrograde aortic collagenase perfusion, according to a method originally published by Zaza et al. (12) with minor modifications. After Ca^{2+} readaptation, isolated myocytes were suspended in 1 mM $CaCl_2$ Tyrode containing gentamycine (10 μg/ml) and stored at room temperature until use. Measurements were performed in rod-shaped, quiescent myocytes with clear-cut striations within 12 hours from isolation.

1.2 Voltage-clamp experiments

The cells were superfused at 2 ml min^{-1} with Tyrode solution containing (in mmol/L): 154 NaCl, 4 KCl, 2 $CaCl_2$, 1 $MgCl_2$, 5Hepes-NaOH and 5.5 d-glucose, adjusted to pH 7.35 with NaOH. The pipette solution contained (mmol/L): 110 potassium aspartate, 23 KCl, 0.4 $CaCl_2$ (calculated free Ca^{2+} of 10^{-7} mol/L), 3 $MgCl_2$, 5 Hepes-KOH, 5 EGTA-KOH, 0.4 GTP-Na salt, 5 ATP-Na salt, and 5 creatine phosphate Na salt, adjusted to pH 7.3 with KOH. Membrane capacitance (78.8 ± 2.5 pF) and series resistance (5.3 ± 0.5 MΩ) were measured in every cell (n =36), the latter was compensated to 80% of its original value (Axon Multiclamp 700A). Potential contamination of I_{Ks} recordings by I_{CaL}, I_{NCX} and I_{Kr} was minimized by performing the measurements in the presence of 5 μmol/L nifedipine and 5 mmol/L Ni^{2+} and 5 μM E-4031. To confirm that the recorded current was I_{Ks}, its complete suppression was verified at the end of each recording by exposure to the selective I_{Ks} blocker HMR1556 (1 μM). All solutions were applied by a fast-switch superfusion system with independent temperature monitoring (8).

The voltage dependency of steady-state activation and activation rate were evaluated by depolarizing steps at variable potentials (3 sec, holding potential -40 mV) followed by repolarization to -30 mV. Steady-state activation was measured from the amplitude of tail

currents measured at -30 mV. The resulting I-V data were fitted by the Boltzmann function to estimate mid-activation potential ($V_{0.5}$, in mV), inverse slope factor (1/S, in mV) and current asymptote (I_{max}, in nA). Activation time constants (τ_{act}) were estimated at various potentials by fitting current onset during the depolarizing steps with the sum of two exponentials. Deactivation time constant (τ_{deact}) was estimated by monoexponential fitting of tail current decay at various membrane potentials (-50 to 0 mV) after a 3 sec depolarizing step to 20 mV. Upon repolarization to -80 mV I_{Ks} tails were too small to be accurately fitted; therefeore, at this potential τ_{deact} was estimated from the envelope of instantaneous current amplitudes in the S1-S2 protocol (see text). Data previously published by our group (8) and obtained under the same conditions of the other protocols, were used for pause-dependency of reactivation.

1.3 I_{Ks} kinetic model and parameters optimization technique

Figure 1S shows the kinetic scheme, developed by Silva & Rudy (9), on which the mathematical model of I_{Ks} is based. Description of this scheme is provided in the published article.

Table 1S shows the expressions describing the voltage-dependency of state transition rates appearing in the scheme of Fig 1S; values of parameters are given in Table 2S. Parameter values were estimated by optimization versus experimental data concerning: steady-state current-voltage relationship, voltage-dependency of activation and deactivation rates, pause dependency of reactivation rate. Model optimization was performed by the Nelder-Mead simplex direct algorithm (7), which identifies parameter values by minimizing the sum of squared differences between predicted and observed data values. Parameter values previously published by Silva and Rudy (9) were used as the initial guess in the optimization procedure for control conditions; the parameters identified by optimization on control data were then used as the initial guess for model optimization on isoprenaline (ISO) data. The optimization process was iterated until a single set of parameters adequate to reproduce all experimental data was identified for each condition (control and ISO).

It is worth noting that there is no direct correspondence between each transition rate and a specific channel gating property. Hence, changes in the parameters of a single transition may affect several gating properties at the same time, thus potentially influencing simulation of all current features. For this reason, parameter identification reflects the result of a global optimization process, based on the whole set of experimental data. Nevertheless, one gating property may constrain an individual transition more than others, thus helping in preliminary

model tuning. In particular, α, β, γ and θ were initially constrained by I_{Ks} activation rates; η and ω by I_{Ks} deactivation rates; θ, β and δ by the steady-state I-V curve, and ψ by the slow component of I_{Ks} activation.

Model and parameter files can be obtained by submitting a request to the authors.

2 Supplement to Results

2.1 Experimental and simulated I_{Ks} recordings

Examples of I_{Ks} recordings in myocytes and their respective model simulations are shown for all experimental conditions in figure 2S for activation, deactivation and pause-dependency of reactivation (S1-S2 protocol). The voltage protocol used for each measurement is shown in the inset of the respective panel.

2.2. Reactivation kinetics: comparison with two H-H type models

The performance the present model and of two Hodgkin-Huxley (H-H) type ones was compared in the simulation of pause-dependency of reactivation rates (S1-S2 protocol). To this end the models were implemented with their original parameters. The results of this analysis are shown in figures 3S and 4S.

In the model by Terrenoire *et al.* (10) I_{Ks} kinetics is modeled as the product of 3 identical gating variables (x); I_{Ks} onset during the activating step is described by a cubic function:

$$I_{Ks}(t) \propto \left(x(0) + (x_\infty - x(0)) \cdot \left(1 - e^{-\frac{t}{\tau_x}} \right) \right)^3 \qquad \text{(eq 1S)}$$

In this context, pause-dependency of reactivation rate is entirely determined by changes in $x(0)$, i.e. the value of the activation variable at the onset of S2. As the S1-S2 intervals shortens below deactivation time $x(0)$ increases, as revealed by the increase in the instantaneous current (Fig 3S middle panels). A further, more subtle, consequence of incomplete deactivation is a small increase in reactivation rate, explained by the fact that the first time derivative of equation 1S still includes the term $x(0)$ in a form adeguate to affect the kinetics of the time-dependent component. However, the resulting pause-dependency of reactivation rate is much smaller than the one observed in experiments and is limited to the

range of S1-S2 intervals encompassing deactivation (Fig. 4S).. While reducing τ_{act} , ISO does not change τ_{deact} at -80 mV; thus, ISO causes a downward shift in the restitution curve without changing its shape appreciably (Fig 4S).

In the model by Imredy *et al.(5)*,I_{Ks} kinetics is represented by the product of 2 non-identical gating variables, x_1 and x_2 , I_{Ks} onset during an activating step is given by:

$$I_{Ks}(t) \propto \left(x_1(0) + (x_{1\infty} - x_1(0)) \cdot \left(1 - e^{-\frac{t}{\tau_{x1}}} \right) \right) \cdot \left(x_2(0) + (x_{2\infty} - x_2(0)) \cdot \left(1 - e^{-\frac{t}{\tau_{x2}}} \right) \right) \qquad \text{(eq 2S)}$$

with $\tau_{x1} >> \tau_{x2}$ at -80 mV ($\tau_{x1} = 1498\,ms, \tau_{x2} = 30\,ms$) (computed from original parameters at 36°) (5). In this case I_{Ks} deactivation is dominated by the fastest closing gate. After 100 ms x_2 is almost completely deactivated so that instantaneous current is visible only at the shortest S1-S2 intervals (Fig. 3S bottom panels); x_1 closes so slowly that it has negligible effects in the range of S1-S2 intervals encompassing restitution. Moreover, the form in which $x_2(0)$ is represented in the derivative of eq 2S makes it ininfluential on the kinetics of reactivation, which is thus completely independent of the S1-S2 interval (Fig 4S) . Also in this case, modification of parameters to fit forskolin-induced changes (5), which recapitulate ISO-induced ones, simply shifts down the reactivation restitution curve without modifying its shape

In summary, depending on the specific formulation of current, H-H –type models may incorporate pause-dependency of reactivation rate in principle; nevertheless, they cannot reproduce experimental data in terms of magnitude and response to ISO. This is because in H-H models pause-dependency of reactivation rate depends uniquely on incomplete diastolic deactivation (*i.e. x* (0) must be > 0 at the onset of S2), which strictly constrains the model output. This is not the case for Markovian models, in which redistribution between sequential closed states can contribute to explain the phenomenon.

3 Supplement to Discussion

3.1 Further I_{Ks} gating features relevant to modelling

I_{Ks} gating has several distinctive features, which deviate from a simple Hodgkin-Huxley scheme and are thus relevant in defining model complexity. Among them, those

detected in the present experiments are the initial delay in the activation time course and pause-dependency of reactivation rate.

Initial delay in activation, originally described by Cole & Moore in giant squid axons (2) and confirmed for heterologously reconstituted (KvLQT1+MinK proteins) channels (11), has been explained by the presence of transitions between closed states preceding channel opening and motivates their inclusion in the model.

According to the Cole & More hypothesis (2), the interval between subsequent activations may affect the initial delay (as also observed in the present experiments), but should not change the rate of the following exponential activation. Thus, pause-dependency of reactivation rate, as observed in the present and previous (8) experiments, deviates from Cole & More predictions. A similar dependency was observed in heterologously reconstituted channels (tested at room temperature) and interpreted as depolarization-induced transition to a faster gating "mode" whose contribution to reactivation depends on the interval between pulses (11). The kinetic scheme for "modal gating" would include two parallel chains of transitions for each channel monomer and a further transition to connect them. The results of the present modelling, based on a single chain of transitions for each monomer, indicate that modal gating is not required to account for pause-dependency of I_{Ks} reactivation rate.

Lack of symmetry between activation and deactivation kinetics at the same potential, a further deviation from Cole & More predictions, observed in reconstituted channels (11), could not be verified in the present experiments; indeed, at the only potential at which they were both measured (0 mV), activation and deactivation rates did not differ significantly. This might either represent a difference in the function of native vs reconstituted I_{Ks} channels, or simply depend on the effect of temperature (35 °C for native channels vs 20 °C for reconstituted channels) on gating kinetics.

3.2 Mechanisms of ISO-induced increase in maximal conductance

In previous models the ISO-induced increase in maximal I_{Ks} conductance was reproduced by an increment in G_{Ks}, which implies an increase in single channel conductance (g_{Ks}), in channel density (σ), or both. Waxing and waning of I_{Ks} modulation by ISO required less than 1 minute in the present experiments, a time course fully compatible with modulation of open probability (P_O), On the other hand, a change in σ would involve modulation of either protein synthesis or trafficking. Whereas regulation of protein synthesis occurs on a time-scale

incompatible with the present findings (4), modulation of endocytic KCNQ1/KCNE1 channel recycling in Xenopus oocyte was found to increase current amplitude several minutes after injection of activated glucocorticoid-inducible kinase 1 (SGK1), without affecting current kinetics. Although the time course of channel recycling modulation might roughly fit with I_{Ks} response to ISO, the latter was also characterized by changes in current kinetics, not expected from a simple increase in channel density. To our best knowledge, receptor-induced modulation of g_{Ks} has never been described in voltage-operated channels (VOCs). A few instances of phosphorylation-induced modulation of unitary conductance do exist, but concern channels other than VOCs (e.g. gap-junctions, AMPA-R, RyR) (1,3,6). Overall, it cannot be ruled out that changes in the $g_{Ks} \bullet \sigma$ product may cooperate with Po changes to I_{Ks} modulation by ISO. Nevertheless, the view that changes in P_o alone may be theoretically adequate to account for the modulation is novel and provides a unitary framework for the interpretation of adrenergic control of I_{Ks}.

SUPPLEMENT TABLES

Table 1S – Model expressions for voltage-dependency of transition rates (s^{-1}). The values of expression parameters ($P_{1\alpha}$ etc.) are reported in Table 2S

Voltage-dependency of transition rates
$\alpha = P_{1\alpha}/(1+\exp(-(V_m-P_{2\alpha})/P_{3\alpha}\cdot F/R/T))$
$\beta = P_{1\beta}/(1+\exp((V_m-P_{2\beta})/P_{3\beta}\cdot F/R/T))$
$\gamma = P_{1\gamma}/(1+\exp(-(V_m-P_{2\gamma})/P_{3\gamma}\cdot F/R/T))$
$\delta = P_{1\delta}\exp(P_{2\delta}\cdot V_m\cdot F/R/T)$
$\eta = (P_{1\eta}-P_{4\eta})/(1+\exp((V_m-P_{2\eta})/P_{3\eta}\cdot F/R/T))+ P_{4\eta}$
$\psi = P_{1\psi}\exp(P_{2\psi}\cdot V_m\cdot F/R/T)$
$\omega = P_{1\omega}\exp(P_{2\omega}\cdot V_m\cdot F/R/T)$

R=8.314 [J/mol/K], F=96485.34 [C/mol], T=310.0 [K], V_m= membrane potential [V]

Table 2S – Model parameters for control (CTRL) and isoprenaline stimulation (ISO).

PARAMETER	CTRL	ISO
$P_{1\alpha}$	8.7743	18.1806
$P_{2\alpha}$	0.0204	0.0318
$P_{3\alpha}$	1.0349	0.9059
$P_{1\beta}$	14.5254	14.4318
$P_{2\beta}$	0.0399	unchanged
$P_{3\beta}$	1.4191	1.4368
$P_{1\gamma}$	747.771	unchanged
$P_{2\gamma}$	-0.1112	unchanged
$P_{3\gamma}$	0.3418	unchanged
$P_{1\delta}$	93.2953	unchanged
$P_{2\delta}$	-0.0695	unchanged
$P_{1\eta}$	55.2459	46.1828
$P_{2\eta}$	-0.0481	-0.048
$P_{3\eta}$	0.714	0.7641
$P_{4\eta}$	3.8883	1.2016
$P_{1\psi}$	0.3215	unchanged
$P_{2\psi}$	0.2529	unchanged
$P_{1\omega}$	1.5922	unchanged
$P_{2\omega}$	-0.8405	unchanged
θ	3.0763	7.3175

SUPPLEMENT FIGURE LEGEND

Fig. 1S – Kinetic scheme of I_{Ks} model. The model contains 15 closed (C1 to C15) states to account for 4 voltage sensors (channel monomers) each undergoing 2 transitions before channel opening. Black closed states C1-C13 with the exception of states inside the gray area represent channels for which the first transition has been completed by only part of the 4 voltage sensors (Zone 2). The remaining states in the gray zone represent channels in which the first transition has been completed by all 4 voltage sensors (Zone 1). There are 2 open states (O1 and O2, white) with no inactivation. Modified from (9).

Fig. 2S – Sample I_{Ks} recordings in myocytes in control and during isoprenaline (ISO). I_{Ks} recordings in myocytes (top) and the respective model simulations (bottom) are shown for each experimental protocol (shown in the inset). A) voltage-dependency of activation (steady-state and kinetics); B) voltage dependency of deactivation kinetics (except at -80 mV).; C) S1-S2 protocol for pause-dependency of reactivation rate (restitution) and deactivation kinetics at -80 mV (envelope test). The voltage protocol used for each measurement is shown in the inset of the respective panel.

Fig. 3S – Comparison with H-H-type models. Simulation of I_{Ks} recordings during the S2 pulse of the S1-S2 protocol in control (left panels) and ISO or forskolin (FSK) (right panels) , The present model (top) is compared to those proposed by, Terrenoire et al. (mid) and by Imredy et al. (bottom).

Fig. 4S – Comparison with H-H-type models.. Reactivation time constants (τ_{react}) in control (thin lines) and ISO (thick lines) conditions are plotted vs S1-S2 intervals for the present model (black lines and data points) and H-H-type models by Terrenoire et al (red lines) and Imredy et al (blue lines) .

Fig. 5S – Model simulation of cycle-length dependency of action potential duration (APD) and its modulation. APD_{90} was measured at steady state during simulated pacing at various CLs under control (thin line), ISO (thick line) and during ISO and 50% reduction of I_{Ks} conductance (dashed line).

SUPPLEMENT FIGURES

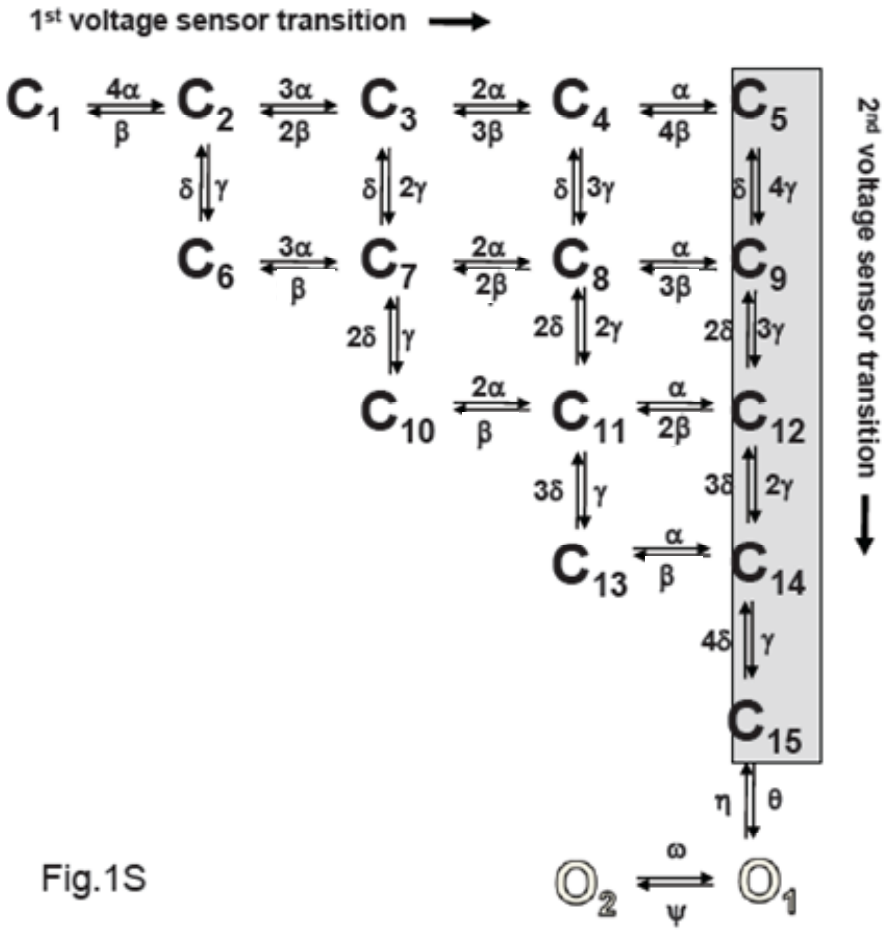

Fig.1S

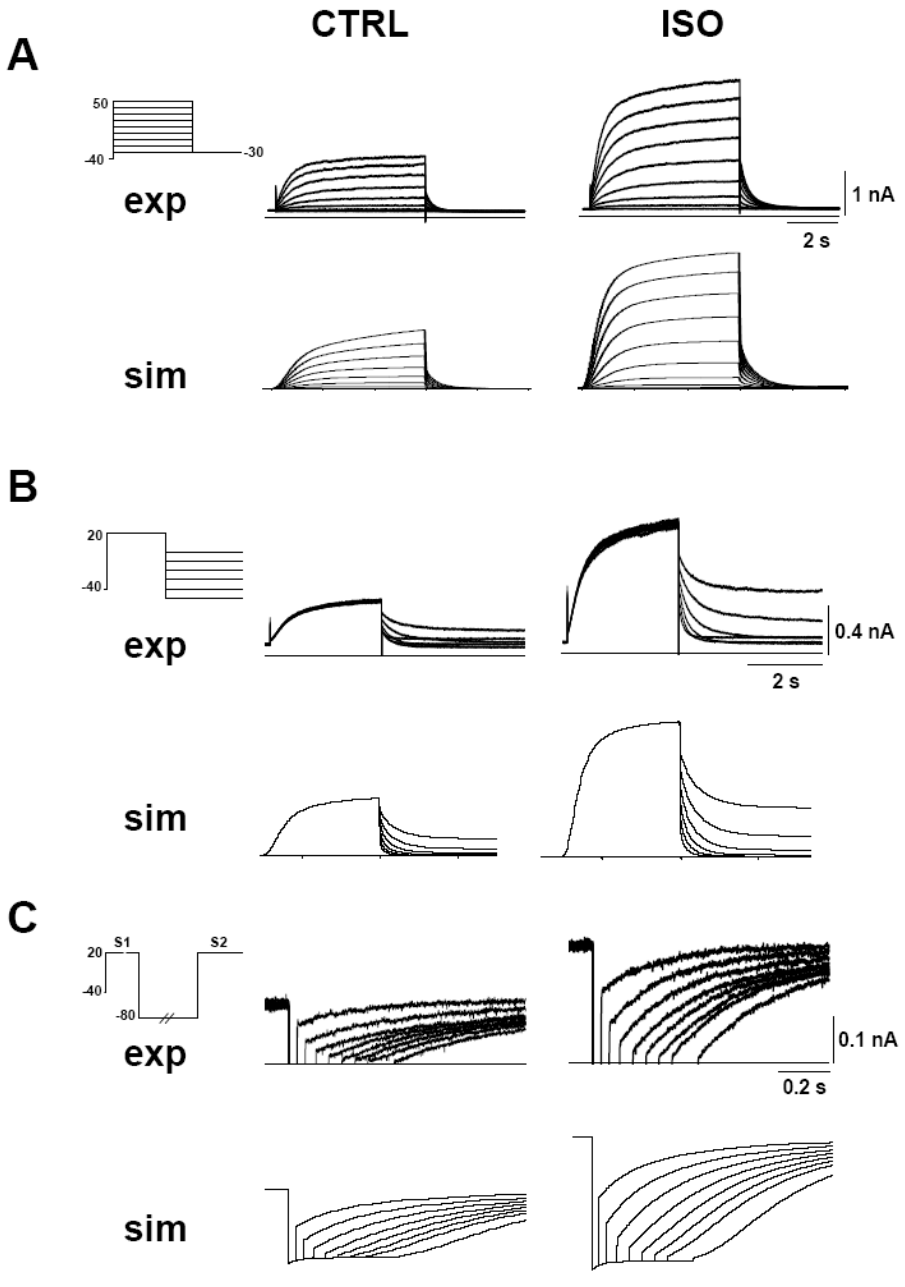
A
CTRL
ISO
50
-40
-30
exp
sim
1 nA
2 s
B
20
-40
exp
sim
0.4 nA
2 s
C
S1
S2
20
-40
-80
exp
sim
0.1 nA
0.2 s

FIG 2S

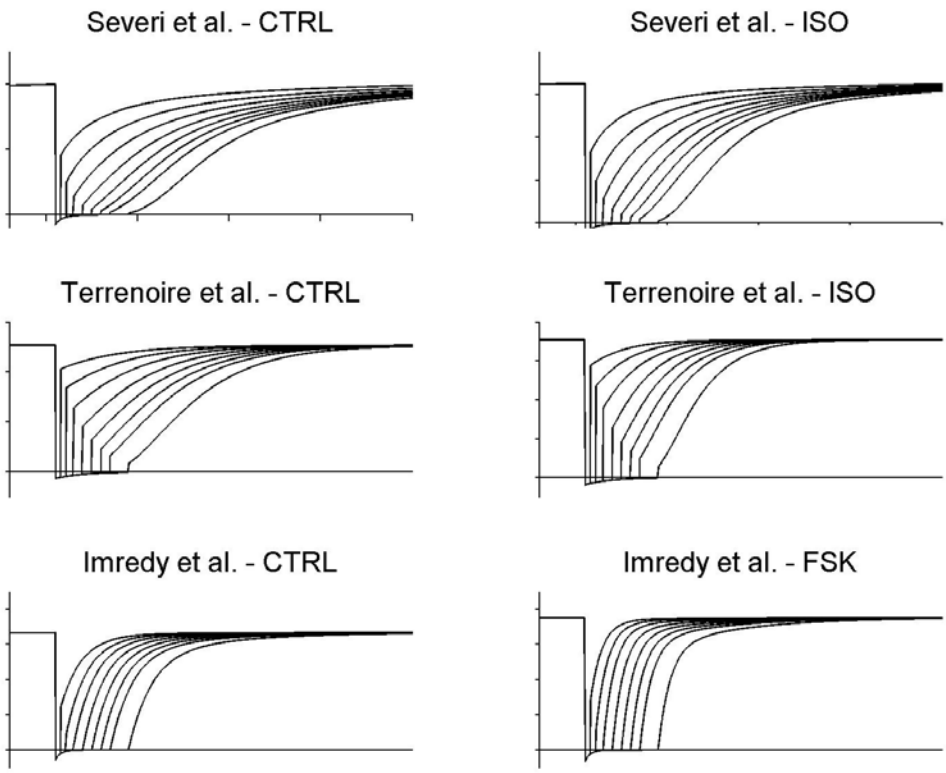
Severi et al. - CTRL
Severi et al. - ISO
Terrenoire et al. - CTRL
Terrenoire et al. - ISO
Imredy et al. - CTRL
Imredy et al. - FSK

FIG 3S

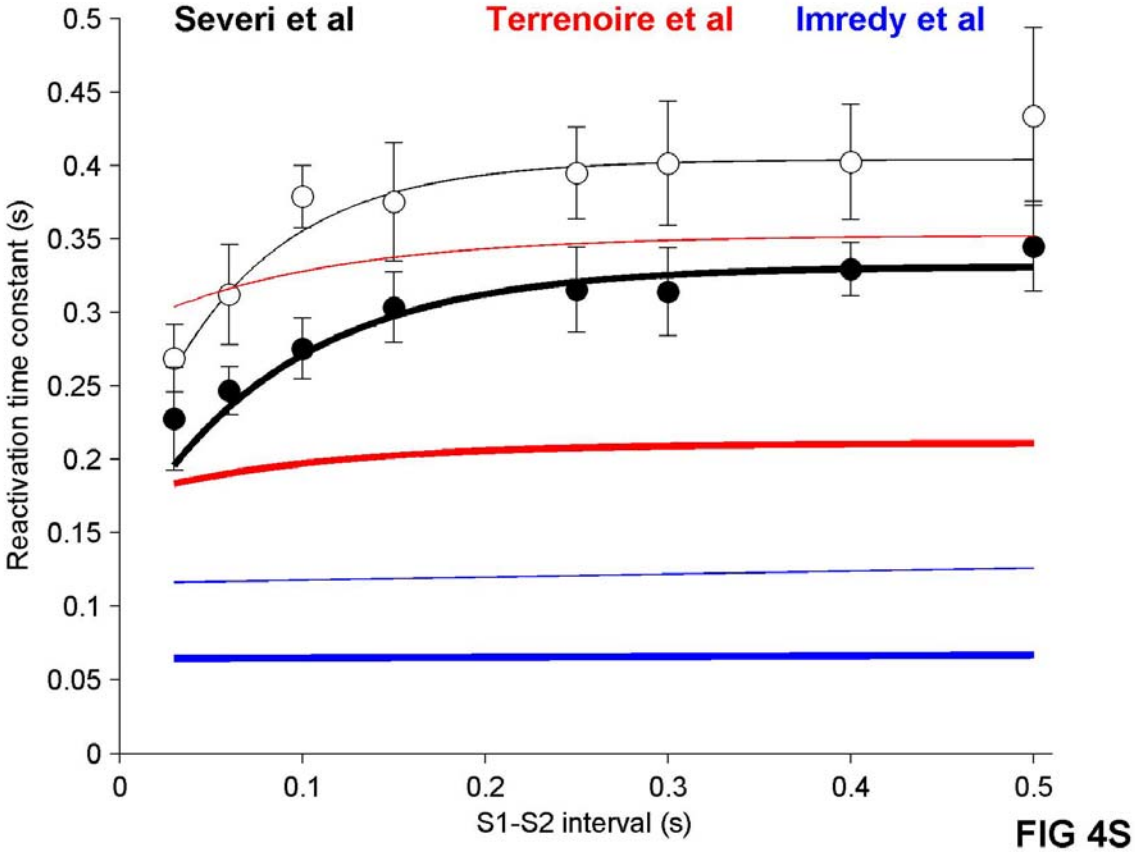
Severi et al
Terrenoire et al
Imredy et al
Reactivation time constant (s)
S1-S2 interval (s)
0.5
0.45
0.4
0.35
0.3
0.25
0.2
0.15
0.1
0.05
0
0
0.1
0.2
0.3
0.4
0.5

FIG 4S

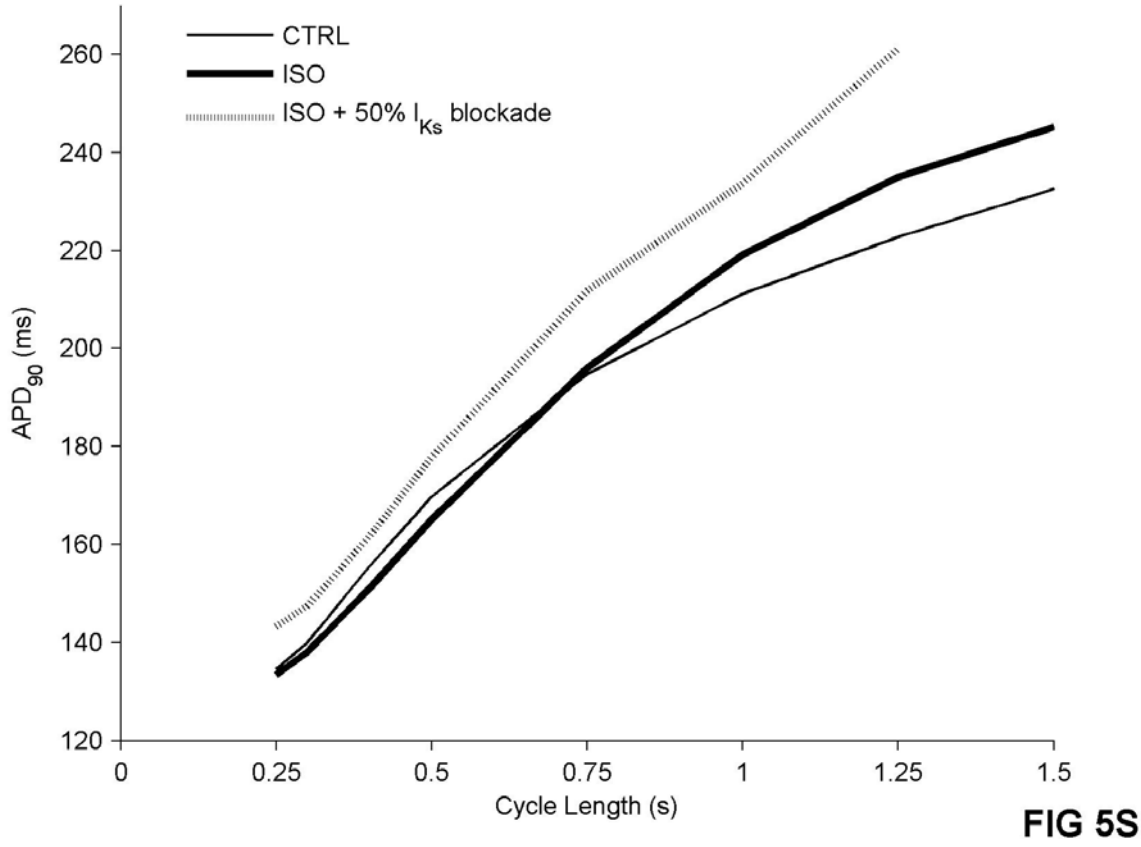

FIG 5S

Reference List

1. Carter,S., J.Colyer, and R.Sitsapesan. 2006. Maximum Phosphorylation of the Cardiac Ryanodine Receptor at Serine-2809 by Protein Kinase A Produces Unique Modifications to Channel Gating and Conductance Not Observed at Lower Levels of Phosphorylation. *Circ Res* 98:1506-1513.

2. Cole,K.S. and J.W.Moore. 1960. Potassium ion current in the squid giant axon: dynamic characteristic. *Biophys. J.* 1:1-14.

3. Derkach,V., A.Barria, and T.R.Soderling. 1999. Ca2+/calmodulin-kinase II enhances channel conductance of alpha-amino-3-hydroxy-5-methyl-4-isoxazolepropionate type glutamate receptors. *Proc. Natl. Acad. Sci. U. S. A* 96:3269-3274.

4. Herve,J.C., M.Derangeon, B.Bahbouhi, M.Mesnil, and D.Sarrouilhe. 2007. The connexin turnover, an important modulating factor of the level of cell-to-cell junctional communication: comparison with other integral membrane proteins. *J. Membr. Biol.* 217:21-33.

5. Imredy,J.P., J.R.Penniman, S.J.Dech, W.D.Irving, and J.J.Salata. 2008. Modeling of the adrenergic response of the human IKs current (hKCNQ1/hKCNE1)stably expressed in HEK-293 cells. *Am. J. Physiol Heart Circ. Physiol* In press.

6. Moreno,A.P., J.C.Saez, G.I.Fishman, and D.C.Spray. 1994. Human connexin43 gap junction channels. Regulation of unitary conductances by phosphorylation. *Circ. Res.* 74:1050-1057.

7. Nelder,J.A. and R.Mead. 1965. A simplex method for function minimization. *Comput J* 7:308-313.

8. Rocchetti,M., V.Freli, V.Perego, C.Altomare, G.Mostacciuolo, and A.Zaza. 2006. Rate-dependency of beta-adrenergic modulation of repolarizing currents in the guinea-pig ventricle. *J. Physiol* 574:183-193.

9. Silva,J. and Y.Rudy. 2005. Subunit interaction determines IKs participation in cardiac repolarization and repolarization reserve. *Circulation* 112:1384-1391.

10. Terrenoire,C., C.E.Clancy, J.W.Cormier, K.J.Sampson, and R.S.Kass. 2005. Autonomic control of cardiac action potentials: role of potassium channel kinetics in response to sympathetic stimulation. *Circ. Res.* 96:e25-e34.

11. Tzounopoulos,T., J.Maylie, and J.P.Adelman. 1998. Gating of I(sK) channels expressed in Xenopus oocytes. *Biophys. J.* 74:2299-2305.

12. Zaza,A., M.Rocchetti, A.Brioschi, A.Cantadori, and A.Ferroni. 1998. Dynamic Ca^{2+}-induced inward rectification of K^{+} current during the ventricular action potential. *Circ. Res.* 82:947-956.